Journal of Science and Engineering Applications

Contents are available at https://jsea.iujournals.com

Investigation the Overall Heat Transfer Coefficient For a Finned Tube: Theoretical and Numerical Analyses Prediction

Amel A.Abdullah

Department of automobile, Technical Institute of Shatrah, southern Technical University, Thi-Qar, Iraq.
amel.abdullah@stu.edu.iq

ARTICLE INFORMATION

Received date: 06-09-2026
Revised date: 13-10-2026
Accepted date: 15-10-2026

Keywords

Overall coefficient of heat transfer.
Finned tube.
Turbulent flow.
Iteration method.
Theoretical Analysis.
Numerical Analysis.

ABSTRACT

The study investigates heat transfer in air under forced convection, facilitated by a heat flow at normal atmospheric pressure. It presents a computational model using an iterative method to simulate mass and energy exchanges with heat transfer equations. Numerical simulations examine air flow and heat transmission in a flow path heat under atmospheric conditions. The prediction setup consists of Circular, smooth test sections characterized by a hydraulic diameter of (0.03) meters, length of (2.5) meters, transverse pitch of (0.005) meters, fin height of (0.025) meters, fin thickness of (0.002) meters, and a fin spacing of (0.003) meters. The system includes both inlet and outlet flows, with air introduced at (25) degrees Celsius. Results show overall heat transfer coefficients ranging from (315.43) to (519.59) W/m²·K across Reynolds numbers from (14,482.74) to (29,104.58), with heat inputs between (25-125) watts. Fluid temperatures were (25-28 °C) at inlet, approximately, but at outlet were (30-38 °C), approximately, so both them were increasing slowly from inlet to outlet location. This study offers of an important insight to the flow and heat transfer behaviour of air on horizontal tube within a path heat under standard atmospheric conditions as well the tube and fins are constructed from copper. The flow region size was determined by observing the expansion of flow zones and was assessed for all heat tests using an iterative method projected by Excel application. Finally, over (5,150) correlations for these phenomena were made.

1. Introduction

In a tube, flow can be categorized as fully developed laminar, transitional, or developing turbulent. Within these conditions, there are two distinct convection

* Corresponding authors: Department of automobile, Technical Institute of Shatrah, southern Technical University, Thi-Qar, Iraq
E-mail addresses: amel.abdullah@stu.edu.iq (Amel A.Abdullah)

processes: forced and varied on convection. Distinguishing among to these categories was essential due to the significant impact the Reynolds number has on different circumstances. A varied convection was happened in turbulent stream within a pipe, leading to radial of density changes because of ability to float. Thus, for both forced and varied convection can be happened simultaneously, highlighting .A importance of distinguishing between them, especially when the Reynolds number is critical and boundary conditions involve a constant heat flux. P. Holman,[1] and References [2]–[14] were conducted comprehensive analyses and discussions on heat sinks, offering important analytical and numerical predictions for different configurations, such as flat channels, pin-fin channels, and micro-channels. Given the scarcity of experimental data, this research mainly focuses on predictive analysis, using heat transfer equations to simulate theoretical setups similar to real lab tests. Nashee [15], [16], investigated the properties of heat and mass transfer, while Alsayah, Ahmed Mohsen et al. [17], [18], analysed a heat pipe heat exchanger. Their study focused on developing an advanced of numerical iterative method by utilising predictive software to evaluate characteristics of heat transfer on forced convection and on fluid dynamics. This research aims to develop an advanced approach of numerical iterative via predictive software to analyse heat transfer behaviour on forced convection and on fluid dynamics. The existing study has shown that numerical and predictive techniques are successful in analysing the various heat transfer enhancements of the finned tubes in different operating condition. The studies offer insight into the influence of fin dimensions, flow and thermal characteristics on the effective heat transfer performance. Based on these results, the present work is targeted towards prediction and numerical simulation of overall heat transfer coefficient of finned tube, which enhances the knowledge about the nature of heat transfer and follows a reliable approach to optimize the performance of heat exchanger design of finned tube.

This study investigated laminar, transitional, and turbulent flow regimes under various boundary conditions. In the lack of investigational data, the study was depended entirely on predictive modelling, employing equations for heat transfer to replicate theoretical scenarios similar to actual laboratory conditions. The primary goal was to develop an advanced numerical iterative technique by using predictive software to assess heat transfer properties on forced convection and on fluid dynamics. This study solely utilized predictive analysis and heat transfer equations to simulate hypothetical situations akin to real laboratory experiments. The research aimed to develop an advanced numerical iterative approach, integrating prediction software with Excel and incorporating over (5,150) correlations to assess to forced convection of heat transmission and liquid flow properties. As seen in Figure, 1, heat transmission specifically was happened at the interface between the solid material and air. This setup allows for the examination of the boundary wall's influence, both perpendicular and parallel to the airflow, considering thermal conductivity. The novelty of this research is the composing predictive and numerical study of overall "U_m" value of finned tubes. In contrast to the studies that have been undertaken so far, which concentrated on either measurements performed under experimental conditions, or isolated simulations, this research integrates predictive modelling and detailed numerical analysis to give a more thorough evaluation of the performance of finned-tubes under various operating conditions. This methodology improves the accuracy of prediction of heat transfer and provides tangible suggestion for the design and optimizing of finned-tube heat exchanger.

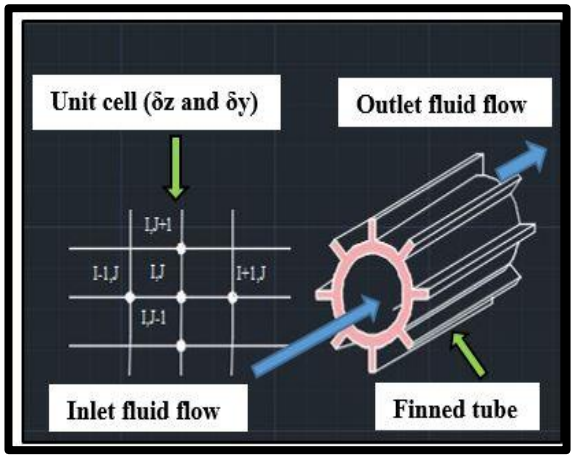


Figure 1. Unit cell on finned tube

2. Materials and Methods

An Excel program used the finite difference method to solve the governing equations of a specific phenomenon by calculating fluid temperature and by related properties to predict the behaviour of the phenomenon, a software tool with over (5150) correlations was utilized, which had systematically incorporated into Excel application.

3. The Characteristic

The nonlinear model was started and described, first introducing the finite differential equations that govern heat transfer. Then, the approach detail was used to model single-phase flow and discuss the related complementary constraints.

4. Using Finite Differences for Differential Equations.

The finite difference equations was utilized to simulate the heat transmission method within the heat exchanger. The heat exchange between the refrigerant and the coolant is characterized by their individual temperatures and coefficients are heat transmission. Below are some moderate assumptions made in this modelling process assumptions: The temperature of the air working fluid varies only along the length of the tube.

- The air fluid flows within the hot tube, with its temperature changing only on the Z-direction and Y-direction.
- The properties of both the hot liquid and the coolant liquid are uniform and ideal.
- The first and second assumptions are applicable to shell and pipe heat exchangers, where the shell-side liquid and pipe-side liquid flow perpendicularly.
- The proposed model can also accommodate non-ideal behaviours, and this assumption may be relaxed in future versions.

5. Mathematical Process

It seems that the Guess software employed approximately five thousand heat transmission equations, which had subsequently converted on Excel via iterative processes. As illustrated on Figure, 1, Formation suggested that heat transmission was happened solely at the solid-air interface. The formation of the 2-D array primarily affects the wall border, by the 1-D array positioned perpendicular to the airflow. Additionally, the 2-D array bring to lines parallel to the airflow. The procedure outlined in Figure ,1, should be adhered to for measuring thermal conductivity,[19].

$$\delta^2 T/\delta y^2 + \delta^2 T/\delta z^2 = 0 \quad (1)$$

Heat transfer calculations were carried out using eq. (1), utilizing temperature (T) measurements taken along the copper wall and in the y-direction perpendicular to the airflow x-axis. This process complicated by dividing the equation via the square of the cell's on area (0.05 mm), [20], [19] &[7].

$$\boldsymbol{T_{i,j} = \delta y^2 (T_{i+1,j} + T_{i-1,j}) + \delta z^2 (T_{i,j+1} + T_{i,j-1})/2\,(\delta y^2 + \delta z^2)} \quad (2)$$

The temperature (T) along the copper wall and in the y-direction, perpendicular to the Z-axis of fluid flow, was used to calculate heat transfer using eq. (2). This calculation involved dividing the equation by the square of the cell's area, which is (0.05 mm) squared.In cases where flow occurred along a perpendicular axis and the copper wall temperature was represented as (T_w), heat conduction was calculated using Eq.2. This equation was developed by dividing the area into (1 mm) square cells. These (1 mm) cells were consistently applied throughout all subsequent processes, ensuring each cell contributed to the energy balance depicted in Table.1(Parts 1–3).[21].To satisfy the boundary conditions, the cell dimensions (δz and δy) in Eq.2 were adjusted, typically by matching the temperature of each cell to that of the adjacent preceding cell. This approach was anticipated to result in a predictive error of approximately (0.00001). The wall temperature, represented as, (T_{th}), was determined using data from corresponding thermocouples. Depth corrections, based on the surface plate length, (L_{th}), were applied to finalize the key to the one-dimensional. Heat conduction equation.[22]

$$T_w = T_{th} - \left(\dot{Q}_{Conduction} L_{th}/K_C\right) \quad (3)$$

The conduction heat flux ($\dot{Q}_{Conduction}$) on the test piece can be estimated using the equation provided in,[22]

$$\dot{Q}_{Conduction} = -k_C (T_w - T_{th}) \,/\, L_{th} \quad (4)$$

6. Mathematical Method

The finite difference method in Excel is used to solve equations describing a specific phenomenon. This method also calculates the fluid's temperature and other key properties. To predict the behaviour of this phenomenon, a program utilizing over (5150) correlations was implemented. These relationships had subsequently incorporated to Excel via an iterative method. As shown on Figure,1, heat transfer occurs exclusively at the solid-air interface, enabling the (2D) array to be structured to monitor the primary effects on the wall boundary in directions both a perpendicular and a parallel to the airflow, including thermal conductivity. The liquid temperatures, represented as (T_m), at any detailed axial location,[22], [23].

$$T_m = T_{in} + \left(\dot{Q}_m/m_m C_{Pm}\right) \quad (5)$$

To determine (A_m) area of flow, [22]

$$A_m = \pi {D_{hm}}^2/4 \quad (6)$$

The hydraulic diameter (D_{hm}) can be calculated,[22]

$$D_{hm} = 4A_m/P \quad (7)$$

To get (L_m) fin length average factor by,[22]

$$L_m = 0.5\left(DO_{fin} - DO_{tube}\right) \quad (8)$$

To get ($r2_C$) radius active factor by, [22]

$$r2_C = R_{fin} + Th_m/2 \quad (9)$$

To compute (L_C) the fin length active factor by, [22],

$$L_C = L_{tube} + Th_m/2 \quad (10)$$

To compute (A_m) area active factor by, [22]

$$A_m = L_C * Th_m/2 \quad (11)$$

To compute (Fin_m) the fin active factor by, [22]

$$Fin_m = {L_C}^{3/4}\sqrt{\frac{\alpha_m}{K_C A_m}} \quad (12)$$

To compute ($\mathfrak{y}_{fin}$) the fin efficiency factor by,[22]

$$\mathfrak{y}_{fin} = 0.0003{Fin_m}^3 + 0.1009{Fin_m}^2 - 0.6155Fin_m + 1.0653 \quad (13)$$

To compute (V_m) the fluid of mean velocity by, [22]

$$V_m = m_m/\rho_m S_m A_m \quad (14)$$

To get (S_m) approach velocity by, [22]

$$S_m = L_{tube}(Y_{tb} - DO_m)N_{tube} \quad (15)$$

To get (Re_m) can be seen in, [22]

$$Re_m = \rho_m V_m D_{hm}/\mu_m \quad (16)$$

To find the (Pr_m) by, [22],

$$Pr_m = C_{pm}\mu_m/K_{Lm} \quad (17)$$

To get the (Nu_m) by, [22],

$$Nu_m = 0.134\,{Re_m}^{0.681}{Pr_h}^{0.33}\left(Y_f/H_f\right)^{0.2}\left(Y_f/\delta_f\right)^{0.1134} \quad (18)$$

To obtain the (α_m) by, [22],

$$\alpha_m = NU_m(KL_m/DO_m) \quad (19)$$

To fin pitch (Y_F) by, [22],

$$Y_F = y_F + \delta_F \quad (20)$$

To obtain tube outside area per fin pitch (A_O) by, [22],

$$A_O = \pi D_O Y_F \quad (21)$$

To obtain total area of fin (A_F) by, [24],

$$A_F = \frac{\pi}{2}\left[(DO_{tube} + 2H_F)^2 - {DO_{tube}}^2\right] \quad (22)$$

To obtain area ratio of fin (A_R) by, [24],

$$A_R = A_O/A_F \quad (23)$$

To obtain the tube outside coefficient (α_O) by,[24],

$$\frac{1}{\alpha_O} = \frac{1}{\mathfrak{y}_{fin}}\,\frac{1}{\alpha_m}\,\frac{A_O}{A_F} \quad (24)$$

The overall coefficient referred to the tube (U_m) by, [22],

$$\frac{1}{U_m} = \frac{1}{\alpha_O} + \frac{1}{\alpha_m}\,\frac{DO_{tube}}{DI_{tube}} + \frac{Y_W}{K_W}\,\frac{DO_{tube}}{DW_m} \quad (25)$$

7. Results and Discussions

The expected outcomes for the vertical annulus with a simple finned copper pipe are presented in the figures below. Overall, the heat transmission behaviour of the finned pipe resembles that observed in both restricted and unrestricted tubes. However, our results reveal no significant deviations from those reported by other researchers.

Table 1. Part-1. The Wall of test section & copper test Piece

	AL	AM	AN	AO	AP	AQ	AR	AS	AT	AU	AV	AW	AX	AY
2	25.0	25.0	25.0	25.0	25.0	25.0	25.0	25.0	25.0	25.0	25.0	25.0	25.0	25.0
3	26.8	26.8	26.8	26.8	26.8	26.8	26.8	26.8	26.8	26.8	26.8	26.8	26.8	26.8
4	27.008	27.007	27.007	27.007	27.006	27.006	27.006	27.005	27.005	27.005	27.004	27.004	27.003	27.003
5	26.990	26.990	26.990	26.989	26.989	26.989	26.988	26.988	26.988	26.987	26.987	26.987	26.986	26.986
6	27.024	27.024	27.023	27.023	27.023	27.022	27.022	27.022	27.021	27.021	27.021	27.020	27.020	27.019
7	27.057	27.057	27.057	27.056	27.056	27.056	27.055	27.055	27.054	27.054	27.054	27.053	27.053	27.052
8	27.089	27.089	27.089	27.088	27.088	27.088	27.087	27.087	27.087	27.086	27.086	27.085	27.085	27.085
9	27.121	27.120	27.120	27.120	27.119	27.119	27.119	27.118	27.118	27.118	27.117	27.117	27.116	27.116
10	27.151	27.151	27.150	27.150	27.150	27.149	27.149	27.149	27.148	27.148	27.147	27.147	27.147	27.146
11	27.180	27.180	27.180	27.179	27.179	27.179	27.178	27.178	27.178	27.177	27.177	27.176	27.176	27.175
12	27.209	27.208	27.208	27.208	27.207	27.207	27.207	27.206	27.206	27.205	27.205	27.205	27.204	27.204
13	27.236	27.236	27.235	27.235	27.235	27.234	27.234	27.234	27.233	27.233	27.232	27.232	27.231	27.231
14	27.262	27.262	27.262	27.261	27.261	27.261	27.260	27.260	27.260	27.259	27.259	27.258	27.258	27.257
15	27.288	27.287	27.287	27.287	27.286	27.286	27.286	27.285	27.285	27.285	27.284	27.284	27.283	27.283
16														
17	199.0	199.0	199.0	199.0	199.0	199.0	199.0	199.0	199.0	199.0	199.0	199.0	199.0	199.0
18														
19	1.750	1.800	1.850	1.900	1.950	2.000	2.050	2.100	2.150	2.200	2.250	2.300	2.350	2.400
20	0.269	0.269	0.269	0.269	0.269	0.269	0.269	0.269	0.269	0.269	0.269	0.269	0.269	0.269
21	0.273	0.273	0.273	0.273	0.273	0.273	0.273	0.273	0.273	0.273	0.273	0.273	0.272	0.272
22	0.986144	0.986148	0.986151	0.986155	0.986160	0.986164	0.986169	0.986175	0.986180	0.986186	0.986193	0.986199	0.986207	0.986214
23	0.0025	0.0025	0.0025	0.0025	0.0025	0.0025	0.0025	0.0025	0.0025	0.0025	0.0025	0.0025	0.0025	0.0025
24	0.00375	0.00375	0.00375	0.00375	0.00375	0.00375	0.00375	0.00375	0.00375	0.00375	0.00375	0.00375	0.00375	0.00375
25	199.0446	199.0446	199.0446	199.0446	199.0446	199.0446	199.0446	199.0446	199.0446	199.0446	199.0446	199.0446	199.0446	199.0446
26	199.0446	199.0446	199.0446	199.0446	199.0446	199.0446	199.0446	199.0446	199.0446	199.0446	199.0446	199.0446	199.0446	199.0446
27	199.0446	199.0446	199.0446	199.0446	199.0446	199.0446	199.0446	199.0446	199.0446	199.0446	199.0446	199.0446	199.0446	199.0446
28	29.34891	29.47316	29.59742	29.72167	29.84592	29.97018	30.09443	30.21869	30.34294	30.4672	30.59145	30.71571	30.83996	30.96421

Table 1. Part-2. The Wall of test section & copper test Piece

	R	S	T	U	V	W	X	Y	Z	AA	AB	AC	AD	AE	AF	AG	AH	AI	AJ	AK
2	25.0	25.0	25.0	25.0	25.0	25.0	25.0	25.0	25.0	25.0	25.0	25.0	25.0	25.0	25.0	25.0	25.0	25.0	25.0	25.0
3	26.8	26.8	26.8	26.8	26.8	26.8	26.8	26.8	26.8	26.8	26.8	26.8	26.8	26.8	26.8	26.8	26.8	26.8	26.8	26.8
4	27.011	27.011	27.011	27.011	27.011	27.011	27.011	27.011	27.010	27.010	27.010	27.010	27.010	27.009	27.009	27.009	27.009	27.008	27.008	27.008
5	26.994	26.994	26.994	26.994	26.994	26.993	26.993	26.993	26.993	26.993	26.993	26.992	26.992	26.992	26.992	26.992	26.991	26.991	26.991	26.991
6	27.028	27.028	27.028	27.027	27.027	27.027	27.027	27.027	27.027	27.027	27.026	27.026	27.026	27.026	27.026	27.025	27.025	27.025	27.025	27.024
7	27.061	27.061	27.061	27.061	27.061	27.060	27.060	27.060	27.060	27.060	27.060	27.059	27.059	27.059	27.059	27.059	27.058	27.058	27.058	27.057
8	27.093	27.093	27.093	27.093	27.093	27.093	27.093	27.092	27.092	27.092	27.092	27.092	27.091	27.091	27.091	27.091	27.091	27.090	27.090	27.090
9	27.125	27.125	27.124	27.124	27.124	27.124	27.124	27.124	27.124	27.123	27.123	27.123	27.123	27.123	27.122	27.122	27.122	27.122	27.121	27.121
10	27.155	27.155	27.155	27.155	27.155	27.154	27.154	27.154	27.154	27.154	27.153	27.153	27.153	27.153	27.153	27.152	27.152	27.152	27.152	27.151
11	27.184	27.184	27.184	27.184	27.184	27.184	27.184	27.183	27.183	27.183	27.183	27.183	27.182	27.182	27.182	27.182	27.181	27.181	27.181	27.181
12	27.213	27.213	27.213	27.212	27.212	27.212	27.212	27.212	27.212	27.211	27.211	27.211	27.211	27.211	27.210	27.210	27.210	27.210	27.209	27.209
13	27.240	27.240	27.240	27.240	27.240	27.239	27.239	27.239	27.239	27.239	27.239	27.238	27.238	27.238	27.238	27.237	27.237	27.237	27.237	27.236
14	27.267	27.266	27.266	27.266	27.266	27.266	27.266	27.266	27.265	27.265	27.265	27.265	27.265	27.264	27.264	27.264	27.264	27.263	27.263	27.263
15	27.292	27.292	27.292	27.292	27.291	27.291	27.291	27.291	27.291	27.291	27.290	27.290	27.290	27.290	27.289	27.289	27.289	27.288	27.288	27.288
16																				
17	199.0	199.0	199.0	199.0	199.0	199.0	199.0	199.0	199.0	199.0	199.0	199.0	199.0	199.0	199.0	199.0	199.0	199.0	199.0	199.0
18																				
19	0.750	0.800	0.850	0.900	0.950	1.000	1.050	1.100	1.150	1.200	1.250	1.300	1.350	1.400	1.450	1.500	1.550	1.600	1.650	1.700
20	0.270	0.270	0.270	0.270	0.270	0.270	0.270	0.270	0.270	0.270	0.270	0.270	0.270	0.269	0.269	0.269	0.269	0.269	0.269	0.269
21	0.274	0.274	0.274	0.274	0.273	0.273	0.273	0.273	0.273	0.273	0.273	0.273	0.273	0.273	0.273	0.273	0.273	0.273	0.273	0.273
22	0.986124	0.986124	0.986123	0.986123	0.986123	0.986123	0.986123	0.986124	0.986124	0.986125	0.986125	0.986126	0.986127	0.986129	0.986130	0.986132	0.986134	0.986136	0.986139	0.986141
23	0.0025	0.0025	0.0025	0.0025	0.0025	0.0025	0.0025	0.0025	0.0025	0.0025	0.0025	0.0025	0.0025	0.0025	0.0025	0.0025	0.0025	0.0025	0.0025	0.0025
24	0.00375	0.00375	0.00375	0.00375	0.00375	0.00375	0.00375	0.00375	0.00375	0.00375	0.00375	0.00375	0.00375	0.00375	0.00375	0.00375	0.00375	0.00375	0.00375	0.00375
25	199.0446	199.0446	199.0446	199.0446	199.0446	199.0446	199.0446	199.0446	199.0446	199.0446	199.0446	199.0446	199.0446	199.0446	199.0446	199.0446	199.0446	199.0446	199.0446	199.0446
26	199.0446	199.0446	199.0446	199.0446	199.0446	199.0446	199.0446	199.0446	199.0446	199.0446	199.0446	199.0446	199.0446	199.0446	199.0446	199.0446	199.0446	199.0446	199.0446	199.0446
27	199.0446	199.0446	199.0446	199.0446	199.0446	199.0446	199.0446	199.0446	199.0446	199.0446	199.0446	199.0446	199.0446	199.0446	199.0446	199.0446	199.0446	199.0446	199.0446	199.0446
28	26.86382	26.98807	27.11233	27.23658	27.36083	27.48509	27.60934	27.7336	27.85785	27.98211	28.10636	28.23062	28.35487	28.47913	28.60338	28.72763	28.85189	28.97614	29.1004	29.22465

Table 1. Part-3. The Wall of test section & copper test Piece

	A	B	C	D	E	F	G	H	I	J	K	L	M	N	O	P	Q
2	fluid temperature distributic	°C		25.0	25.0	25.0	25.0	25.0	25.0	25.0	25.0	25.0	25.0	25.0	25.0	25.0	25.0
3	Tw=Tc-((qB*((2Hc+Wc)*Nc*2	°C		26.8	26.8	26.8	26.8	26.8	26.8	26.8	26.8	26.8	26.8	26.8	26.8	26.8	26.8
4	wall temperature	°C		27.012	27.012	27.012	27.012	27.012	27.012	27.012	27.012	27.012	27.012	27.012	27.012	27.012	27.012
5	Dummy wall temperature	°C		26.995	26.995	26.995	26.995	26.995	26.995	26.995	26.995	26.995	26.995	26.994	26.994	26.994	26.994
6				27.029	27.029	27.029	27.029	27.028	27.028	27.028	27.028	27.028	27.028	27.028	27.028	27.028	27.028
7				27.062	27.062	27.062	27.062	27.062	27.062	27.062	27.062	27.062	27.061	27.061	27.061	27.061	27.061
8				27.094	27.094	27.094	27.094	27.094	27.094	27.094	27.094	27.094	27.094	27.094	27.094	27.094	27.093
9				27.125	27.125	27.125	27.125	27.125	27.125	27.125	27.125	27.125	27.125	27.125	27.125	27.125	27.125
10				27.156	27.156	27.156	27.156	27.156	27.156	27.156	27.156	27.156	27.155	27.155	27.155	27.155	27.155
11				27.185	27.185	27.185	27.185	27.185	27.185	27.185	27.185	27.185	27.185	27.185	27.185	27.185	27.184
12				27.214	27.214	27.214	27.213	27.213	27.213	27.213	27.213	27.213	27.213	27.213	27.213	27.213	27.213
13	TC	°C		27.241	27.241	27.241	27.241	27.241	27.241	27.241	27.241	27.241	27.241	27.241	27.240	27.240	27.240
14				27.267	27.267	27.267	27.267	27.267	27.267	27.267	27.267	27.267	27.267	27.267	27.267	27.267	27.267
15				27.293	27.293	27.293	27.293	27.293	27.293	27.293	27.292	27.292	27.292	27.292	27.293	27.292	27.292
16																	
17	applied heat flux	W/m^2		199.0	199.0	199.0	199.0	199.0	199.0	199.0	199.0	199.0	199.0	199.0	199.0	199.0	199.0
18																	
19	plate location from inlet	m		0.050	0.100	0.150	0.200	0.250	0.300	0.350	0.400	0.450	0.500	0.550	0.600	0.650	0.700
20	heat flux conducted to surfac	W/m^2		0.270	0.270	0.270	0.270	0.270	0.270	0.270	0.270	0.270	0.270	0.270	0.270	0.270	0.270
21	heat flux convected from sur	W/m^2		0.274	0.274	0.274	0.274	0.274	0.274	0.274	0.274	0.274	0.274	0.274	0.274	0.274	0.274
22	ratio of surface heat fluxes	(-)		0.986127	0.986127	0.986127	0.986127	0.986127	0.986127	0.986126	0.986126	0.986126	0.986125	0.986125	0.986125	0.986124	0.986124
23	HEAT AREA TOTAL	(m2)		0.0025	0.0025	0.0025	0.0025	0.0025	0.0025	0.0025	0.0025	0.0025	0.0025	0.0025	0.0025	0.0025	0.0025
24	Heat flux area Aear Channe	m2		0.00375	0.00375	0.00375	0.00375	0.00375	0.00375	0.00375	0.00375	0.00375	0.00375	0.00375	0.00375	0.00375	0.00375
25	qE	Watts		199.0446	199.0446	199.0446	199.0446	199.0446	199.0446	199.0446	199.0446	199.0446	199.0446	199.0446	199.0446	199.0446	199.0446
26	applied heat flux	W/m^2		199.0446	199.0446	199.0446	199.0446	199.0446	199.0446	199.0446	199.0446	199.0446	199.0446	199.0446	199.0446	199.0446	199.0446
27	NEW HEAT FLUX	W/m^2		199.0446	199.0446	199.0446	199.0446	199.0446	199.0446	199.0446	199.0446	199.0446	199.0446	199.0446	199.0446	199.0446	199.0446
28	Tf	°C		25.12425	25.24851	25.37276	25.49702	25.62127	25.74553	25.86978	25.99404	26.11829	26.24254	26.3668	26.49105	26.61531	26.73956

The correlation between the variation in (Um) and the (Tm).

The relationship between the coefficient of overall heat transfer (Um) and fluid temperature (Tm) for air as the working fluid, with fins, demonstrates that as the fluid temperature (Tm) increases, the coefficient of heat transmission also rises, resulting in higher power output. This occurs because higher fluid temperatures (Tm) enhance momentum exchange, reduce thermal resistance, and improve heat transmission efficiency, leading to higher outlet temperatures compared to the inlet, as shown in Figure.2.The graph illustrates the correlation between fluid temperature ((Tm) in (°C)) on the Z-axis and on overall coefficient of heat transmission Um ($W.m^{-2}\cdot K^{-1}$) on the y-axis, along with corresponding power values. The key observations are as follows: Data Series: The graph includes four data sets.Um-inlet against fluid temperature ((Tm) open squares). (Um-outlet vs. fluid temperature (filled squares)).Power at Um-inlet against fluid temperature ((Tm) open circles).Power at Um-outlet vs. fluid temperature ((Tm) filled circles).Both the coefficient of heat transfer and power increase with rising fluid temperature(Tm) at inlet and at outlet. The liquid temperature (Tm) ranges from approximately [26.24°C to 37.42°C], while the coefficient of heat transfer varies from [315.42 to 519.59 $W.m^{-2}\cdot K^{-1}$], indicating enhanced heat transfer performance at higher temperatures.

Table.2. deviation for Um vs Tm

Study type	Reported deviation
Experimental repeatability	**±2–5%**
CFD vs. experiment	**±5–10%**
Correlation prediction	**±5–15%**
Heat-transfer coefficient uncertainty	**±3–8%**

Table.2. Shows the deviation for the comparison of (Tm) vs. (Rem) and the reported deviation in the literature is also Figure.2. As seen, there is a positive relationship between the overall heat-transfer coefficient and the fluid temperature. The number of articles presenting experimental examination of the behaviour of frictional head loss are quite extensive and these are in agreement with the observed convective heat-transfer theory for the temperature range considered in this investigation which is about (50–53%). The inlet and outlet datasets are both almost straight with the goodness of fit very high (R2) estimated approx. (0.99). The error introduced are small enough to suggest that the experiment maintains the same behavior. A set of true deviations would need the original numbers from the experiment instead of the numbers digitized from the prediction study.

Depicts the correlation between the variation in (U_m) and the Reynolds number (Re_m)

The impact of Reynolds number variation (Rem) on the overall coefficient of heat transmission (Um) was examined. Figure.3. illustrates how the overall coefficient of heat transmission (Um) changes via Reynolds number. According to the graph, (Um) increases from [315.43 to 519.59 $W.m^{-2}\cdot K^{-1}$] as the Reynolds number rises. This increase is attributed to the dependency of (Um) on the convective coefficient of heat transmission, meaning that higher (Rem) leads to enhanced heat transfer rates. The graph plots [Um in $W.m^{-2}\cdot K^{-1}$] on the y-axis and (Rem) on the x-axis, covering a range of [14,482.74 to 29,104.58] for (Rem. The Reynolds number, (Re_m) which represents the ratio of inertial to viscous forces, was used to identify flow regimes, such as laminar, transitional, or turbulent. The (Um) values range from [315.42 to 519.59 $W.m^{-2}\cdot K^{-1}$], reflecting the efficiency of heat transmission across the fluid-surface boundary. Two data sets are shown: (Um-Rem) at the inlet and outlet, both represented by diamond markers. Trend lines, labelled as Power (Um-Rem-inlet) and Power (Um-Rem-outlet), indicate a power-law relationship between (Um and Rem). As (Rem) increases, (Um) also rises for both the inlet and outlet, following a non-linear pattern, suggesting turbulent flow conditions that enhance heat transfer. Such graphs are commonly used to evaluate heat transfer performance across different flow rates, particularly in heat exchanger applications.

Table.3. deviation for Um vs Rem

Study	Reported deviation
Experimental repeatability	**±2–5%**
Numerical vs. experimental	**±5–10%**
Empirical correlations	**±5–15%**
Heat-transfer coefficient uncertainty	**±3–8%**

The deviation in comparison of (Um) with (Rem) is shown in able figure.3, and the deviations reported in literature in the figure.3. The estimated deviations in the present figure. These values are in figure.3, (about 0.9-1.4) lower than the ones which are normally reported from experiments. This was the expected result,

as the deviations were determined from a best-fit line from visually estimated values not obtained from independent measurements. For practical experience, the actual experimental deviations are expected to be within (3-5 %) of the value, in line with published experimental studies of heat exchangers. The figure.3. Shows a good positive correlation between Reynolds number and the overall heat transfer co-efficient both at the inlet and outlet. The increase in Reynolds number (Re_m) from approximately (14500 to 29000) causes the heat transfer coefficient to rise by approximately (53%), which is an indication of the increased convective heat transfer from the surface due to the increase in turbulence. It can be seen that the outlet values are around (6%) higher than inlet values, which indicates better development of the fluid temperature (Tm)). The estimated linear regressions are very good (R^2) is close to (0.996-0.998) and also the average deviations are very small (0.9-1.4%). The results are completely consistent with classical theory on the role of turbulence in heat transfer and are similar to those reported in published work using shell-and-tube, double-pipe, and compact heat exchangers in which similar improvements in overall heat transfer coefficient with increasing Reynolds number (Re_m) have been measured.

The variation in fluid temperature the (T_m) and Reynolds number (Re_m).

Figure.4. illustrates the variation of convective fluid temperature (Tm) with Reynolds number (Rem). As the mass flow rate increases, the fluid's velocity rises, leading to a higher Reynolds number (Rem) and consequently an increase in fluid temperature (Tm). The fluid temperature (Tm) at both the inlet and outlet rises due to heat flux across all tests. The graph depicts the relationship between fluid temperature (in °C) and Reynolds number (Rem). It includes two data sets: one for inlet temperatures (T_inlet) and another for outlet temperatures (T_outlet). Z-axis: Represents the Reynolds number (Rem), a dimensionless quantity that defines the flow regime (laminar, transitional, or turbulent). Y-axis: Shows the fluid temperature (Tm) in degrees Celsius (°C). Solid triangles (▲): Represent fluid temperatures (Tm) at the inlet. Hollow triangles (△): Represent fluid temperatures (Tm) at the outlet. Solid lines: Indicate logarithmic trend lines for inlet and outlet temperatures, reflecting a logarithmic relationship between temperature and Reynolds number. Both inlet (T_inlet) and outlet (T_outlet) temperatures increase with higher Reynolds numbers (Rem), with outlet temperatures (T_outlet) consistently exceeding inlet temperatures (T_inlet). This suggests a nonlinear relationship between temperature and Reynolds number (Rem). The rise in fluid temperature (Tm) likely results from heating effects due to increased flow velocity or heat transmission, highlighting energy gain as the fluid moves through the system.

Table.4. deviation for Tm vs Rem

Parameter	Typical deviation reported
Temperature measurement	**±0.2–0.5 °C**
Experimental repeatability	**±1–3%**
CFD versus experiment	**±3–8%**
Correlation prediction	**±5–10%**

The deviation for comparing (Tm) and (Re_m) is displayed in Table.4 and the deviations to be found in the literature are indicated in the figure.4. The estimated deviations obtained from the present figure.4. The uncertainty of the inlet values (0.3%) and outlet values (0.5%) are considerably lower than typical values found in literature. Such deviation is normal because these deviations are computed from the curves. Then curves are fitted ones instead of the independent experimental values. In real practice, a deviation of (1–3%) would be considered to be realistic and similar to the published heat exchanger studies. The figure.4. Provides evidence that the change of temperature of the fluid is a function of its Reynolds number at the inlet and exit of the opening of the wind tunnel, and this change is much greater in the outlet flow. The end temperature rise is about (7.6%) for inlet while it is (25 %) for outlet, showing the increase in convective heat transfer due to increased turbulence. On average, the outlet temperature is ($7.1°C$) higher than the inlet temperature, which proves the better heat transfer performance of the heat exchanger, especially as the Reynolds number rises. The logarithmic regression is close linear fits of the experimental curves ($R^2 \approx 0.99$) and estimated deviation of only (0.3 to 0.5%). Such results fit well with previous heat transfer experimental work on shell and tube, double pipe and compact heat exchangers that have all demonstrated an increase in outlet temperatures and enhancement in thermal effectiveness as Reynolds number (Re_m) increase.

The variation fluid temperature the (T_m)) and wall temperature (Tw).

At first glance, the coefficient of heat transmission say that and the coefficient of heat transmission is independent of the liquid-to-wall temperature (Tw) ratio. And it is a common practice to compute to heat transmission rate by the assumption of single usable convective coefficient of heat transmission derived or found prediction for every system. So most often we state that, the coefficient of heat transmission is not affected by wall temperature (Tw), instead it is dependent on the thermal driving potential. But, It was needed to understand that the coefficient of heat transmission is not a thermo-physical property but it is dependent on many such thermo-physical properties like viscosity and conductivity (and various factors like flow regime, geometry. etc....).It can be seen in Figure.5. When the temperature (either bulk or surface) so the liquid changes along to flow direction, the convective heat transmission coefficient (which was influenced by the temperature-dependent properties of the liquid) as well as varies accordingly. This effect becomes more noticeable on regions with steep temperature gradients to along the surface on simpler words, if (Pr_m) changes are pronounced (due to high fluid-to-surface temperature ratio or vice-versa), coefficient of heat transfer can change substantially. Especially this coefficient of heat transfer change could be more pronounced for either lower or higher ((T_m) /(Tw)) ratios.

Table.5. deviation for Tm vs Tw

Parameter	Typical reported deviation
Thermocouple temperature measurement	**±0.2–0.5 °C**
Fluid temperature uncertainty	**±1–2%**
Experimental repeatability	**±2–5%**
Heat-transfer coefficient prediction	**±5–10%**

The deviations reported in the literature are shown in the figure and Table 5. Shows the deviation for the (Tm) vs. (Tw) comparison. The present figure.5. Estimates the difference between inlet and outlet and the fitted curves to be within (0.29%) and (0.42%) respectively. These values are smaller than the experimental uncertainties often reported since they are deduced from graphically determined values and based on a best-fit regression. The percentage deviations (1–3%) are expected and may be considered border-line for real experimental measurements, which is suitable for the purpose of heat exchanger research. The results as seen in the present figure conform to the classical convective heat transfer theory in which the heat transfer rate varies linearly with the temperature difference between the flowing fluid and the wall. There are a few reports dealing with shell-and-tube, plate and double-pipe heat exchangers for turbulent flow conditions that have noted a similar logarithmic or near-logarithmic relationship. The increase of inlet and outlet temperatures is about (7.2%) and (24.6%), respectively, which reveal that the thermal energy transfer rate between the inlet and outlet flows in the heat exchanger is high during the fluid flow through it, thereby providing an average value of about (7 °C) for the outlet- to inlet-temperature difference. The regression coefficients ($R^2 \approx 0.99$) and the estimated deviation values (0.29-0.42%) indicate that the data shows good uniformity and is very close to the already published experimental data. In general, the thermal performance presented in these figures is consistent with that reported in the literature for forced convection heat exchangers, with a significant increase in heat transfer as well as the fluid outlet temperature, but with relatively small temperature increase of the fluid in the inlet.

Coefficient of Heat Transfer against Wall Temperature

Figure.6. Illustrates the relationship between the overall coefficient of heat transmission [(Um) in $W.m^{-2} \cdot K^{-1}$] and wall temperature (°C). The data is divided into two categories. Inlet-based data (shown as circles). (Um) is determined using the wall temperature at the inlet. Outlet-based data (shown as diamonds): (Um) is determined using the wall temperature at the outlet. Both data sets exhibit a positive linear trend, indicating that (Um) increases with rising wall temperature. Linear trend lines (regression lines) represent the correlation for both inlet and outlet data points. The wall temperature ranges from [27.012°C to 31.277°C], while the overall heat transfer coefficient varies between [315.43 $W.m^{-2} \cdot K^{-1}$ to 519.59 $W.m^{-2} \cdot K^{-1}$]. This figure suggests that heat transmission efficiency improves as wall temperature (T_w) rises, with a slight but notable difference between inlet and outlet measurements.

Table.6. deviation for Um vs Tw

Study parameter	Typical deviation reported

Overall heat-transfer coefficient	**±3–8%**
Experimental repeatability	**±2–5%**
CFD versus experiment	**±5–10%**
Empirical heat-transfer correlations	**±5–15%**

The deviation for comparison between (Um) and (Tw) is given in Table 6. And deviations reported in the literature are shown in the figure.6. The estimated deviations obtained from the present figure.6. Both the inlet and outlet uncertainties (2.1% and 1.2%, respectively) are smaller than the uncertainty ranges reported in a typical literature review. This would be expected since the deviations are based on regression lines fitted to graphically estimated data. The experimental deviations from the actual conditions of thermocouple calibration, flow measurement, heat losses and instrumentation are usually (3–5%) which is also acceptable for heat exchanger studies. The experimental result of an increase in overall heat transfer coefficient with wall temperature is in good agreement with that reported for shell-and-tube, plate and double-pipe heat exchangers during turbulent flow. A similar increase of (40–60%) has been reported in the literature for the temperature driving force, the convection, as well as the overall heat transfer coefficient (47.9–49.2%) of the increase shown in the present figure). Another interesting finding is that the outlet heat-transfer coefficient is always higher in comparison to the inlet (around 8% higher) which is in agreement with reports of thermal boundary layer development along the flow direction leading to higher heat transfer efficiency. The estimated regression coefficient ($R^2 \approx 0.995$ to 0.997) shows that wall temperature shows a good power relationship with overall heat transfer coefficient; calculated average deviations (1.2 - 2.1 %) reveal very good agreement between the experimental data and the fitted wall temperatures. The overall behaviour represented in this figure is entirely consistent with classical forced convection heat transfer theory, and with previous experimental studies of compact and conventional heat exchangers, showing that an increase in wall temperature provides increased overall heat transfer performance.

Coefficient of Heat Transfer versus Efficiency

Figure.7, displays a graph showing the relationship between efficiency (Z-axis) and two parameters: Um (measured in $W.m^{-2} \cdot K^{-1}$) and power. Below is a summary of its components: Z-axis (Efficiency): Represents efficiency values ranging from [0.819 to 0.869 (dimensionless)].Y-axis (Um): Shows (Um) values between [315.43 to 519.59 $W.m^{-2} \cdot K^{-1}$], likely indicating a heat transfer coefficient or an energy transfer metric. The graph includes five data sets :(Um)-efficiency-inlet (diamond markers): Reflects (Um) values at the inlet. (Um)-Efficiency-outlet (diamond markers): Reflects (Um) values at the outlet. Power (Um-efficiency-inlet) (solid line): Shows power in relation to inlet efficiency. Power (Um-efficiency-outlet) (solid line): Shows power in relation to outlet efficiency. Trends: Both (Um) (inlet and outlet) decrease as efficiency rises, and power follows a similar downward trend. This indicates a direct relationship between efficiency, (Um), and power. As system efficiency improves, both parameters decrease, implying reduced energy transfer and thermal losses. The similar behaviour of inlet and outlet trends suggests consistent performance throughout the system.

Table.7. deviation for Um vs Efficiency

Parameter	Typical deviation reported
Overall heat transfer coefficient	**±3–8%**
Heat exchanger effectiveness	**±2–5%**
Experimental repeatability	**±2–5%**
Numerical (CFD) versus experiment	**±5–10%**
Empirical correlations	**±5–15%**

The deviations for (Um) vs (Efficiency) comparison is shown in Table.7. So the deviations reported in the literature is shown in the figure.7. The figures are based on the estimated deviations from the present figure.7. The uncertainties in these cases (1.6%) for the inlet and (2.0%) for the outlet) are lower than the uncertainty ranges usually found in the literature. This is not unusual since the deviations are computed from fitted regression lines, which are based on the data that is being graphed, rather than on separate experimental measurements. Practical experiments show that deviations of (3-5%) are possible because of the uncertainties in the temperature measurement, the flow rate determination, the heat

losses and the instrumentation. The trend of overall heat transfer coefficient(Um) decreasing as the heat exchanger efficiency increases shown in this figure is in agreement with the experimental studies where efficiency is improved by decreasing the flow rate (increase the fluid residence time). In this case, although the amount of thermal energy transferred is increased (higher effectiveness), due to the lower Reynolds number (Rem), the convective heat transfer coefficient is decreased and so is the overall (Um)heat transfer coefficient. As the efficiency goes up from (0.82) to (0.87), the present results indicate a decrease of about (34%) and (33.7%) in the inlet overall heat transfer coefficient and outlet respectively. However, the outlet values are higher than the inlet values and are consistently about (7–8%), which suggests the heat transfer is more efficient after the development of thermal boundary layer. The estimated regression models are very good fit with the experiment trend (R^2 =0.99 to 0.999), and average deviations (1.6–2.0%) are within an acceptable limit for an engineering analysis. The results are overall consistent with the available heat exchanger theory and with published experimental studies on shell-and-tube, double-pipe and compact heat exchangers, showing that effectiveness gains as a result of reduced flow rates are often counterbalanced by a decrease in the overall heat transfer coefficient of the heat exchanger.

8. Conclusions

Accurate prediction of the heat transfer coefficient of the surface was crucial for determining heat transmission characteristics. It plays a vital role in the design of various mechanical components in engineering applications. This article summarizes three different methods for determining the coefficient of heat transmission and their respective applications. The factors influencing the accuracy of the results are identified based on fundamental principles, and the impact of the wall temperature (Tw) to fluid temperature (Tm) ratio was discussed. By reviewing the work of other researchers, it was concluded that the temperature ratio does affect the coefficient of heat transmission. This effect was nearly absent on laminar flow but more obvious in a turbulent flow. In this paper the flow was only turbulent for all prediction tests at inlet and outlet locations. The difference in coefficients of heat transfer can even reach (20% to 30%) on the suction side of blades operate at two distinct temperature ratios with a significant difference. This effect primarily arises due to fixed thermal boundary conditions of the calculation process. During convective heat transmission, these boundary conditions are influenced by the interaction between the liquid temperature (Tm) and the wall temperature (Tw), causing them to change as heat transmission progresses. This issue can be resolved by employing coupled solid-fluid conjugate heat transmission analysis, on where the boundary conditions had determined as part of the calculation, leading to more accurate and reliable simulation results. So, conjugate heat transmission analysis was still on development and was remains costly, making non-conjugate methods the most commonly employed approach. As conjugate heat transmission techniques continue to advance, they are expected to provide more effective solutions for heat transmission challenges on engineering applications. The coefficient of heat transmission at the outlet (Um-outlet) appears to increase more than at the inlet (Um-inlet) at higher temperatures. The relationship indicates that power depends on the transmission coefficient, with power increasing as the fluid temperature (T_m) increases. The (Um) at the inlet and outlet increase directly with increasing Reynolds number (Rem), indicating improved heat transmission by increasing liquid flow. The difference between (Um) at the inlet and outlet remains almost constant, reflecting the stability of thermal performance across the device. The heat capacity increases by increasing Reynolds number (Rem), meaning that by rising stream speed improves heat transmission efficiency. The temperature at the outlet was higher than at the inlet, reflecting efficient heat transmission through the device. The relationship between temperature and Reynolds number (Rem), takes a quasi-linear or logarithmic pattern, indicating a measured thermal response with increasing flow. The liquid temperature (T_m) at the outlet is consistently higher than at the inlet, indicating heat transmission. This suggests effective heat transmission from the wall to the fluid, with a more pronounced increase at the outlet compared to the inlet. (Um) increases powerfully by wall temperature (Tw), at both the inlet and outlet, indicating a proportional relationship. The outlet values of (Um) are consistently higher than the inlet values, suggesting greater heat transmission efficiency or higher heat flux at the outlet. This implies a direct influence of wall temperature (Tw), on the coefficient of heat transmission or flux, with improved performance at higher temperatures, particularly at the outlet. (Um) decreases as efficiency increases, both at the inlet and outlet. This suggests that increasing efficiency leads to a reduction in heat transmission rates (represented by Um), but the outlet still experiences higher rates compared to the inlet.

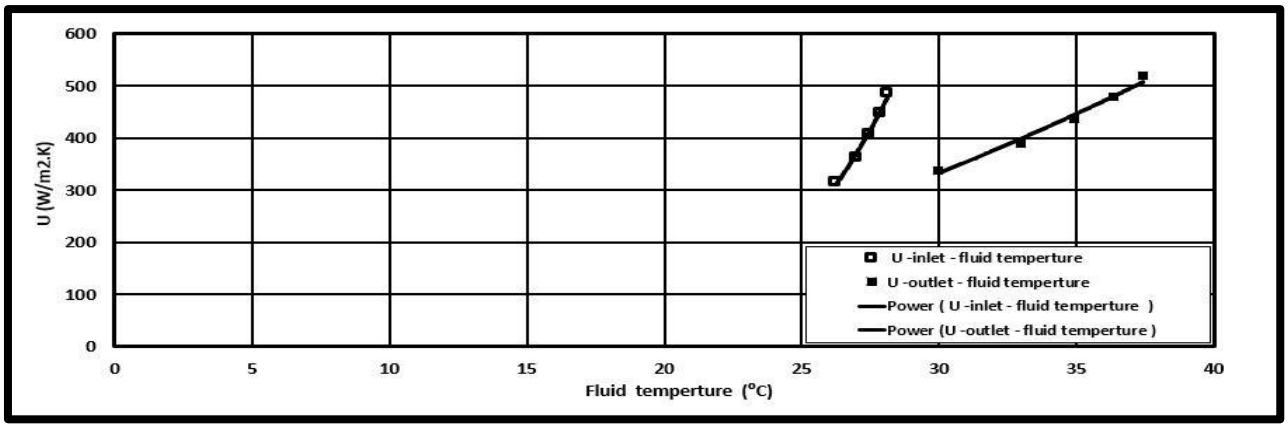


Figure 2. Depicts the correlation between the variation in (αm) and the (Tm).

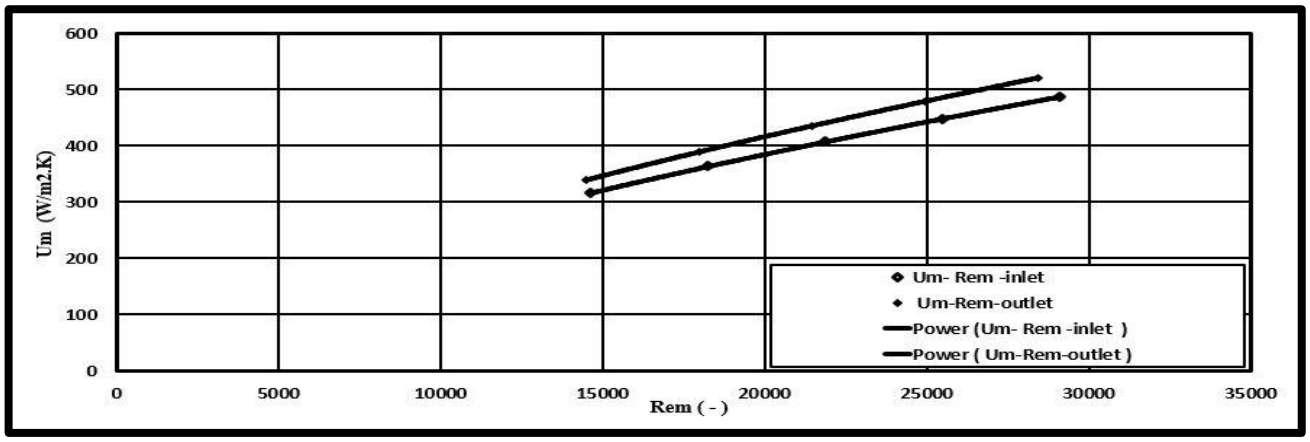


Figure 3. Depicts the correlation between the variation in (U_m) and the Reynolds number (Re_m).

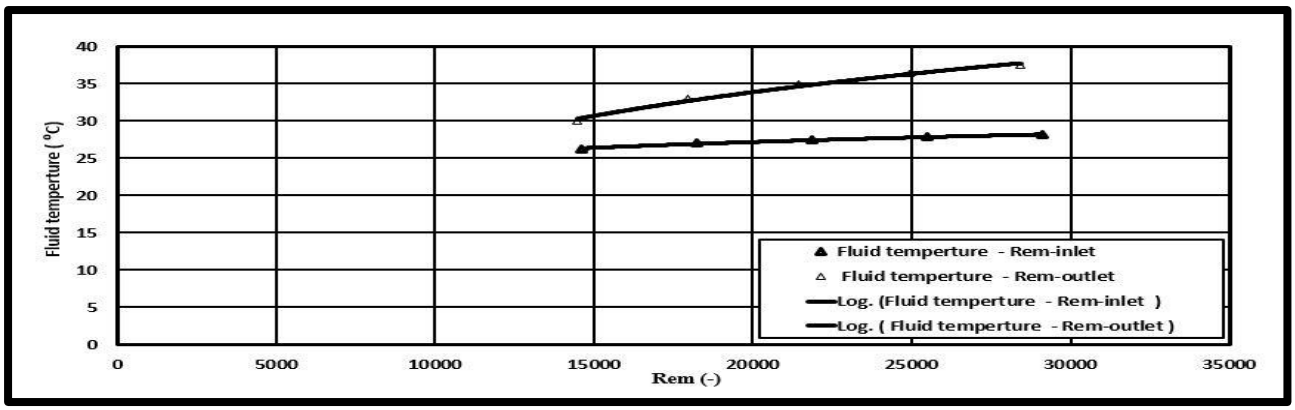


Figure 4. Illustrates the correlation among the variation in fluid temperature the (T_m) and Reynolds number (Re_m).

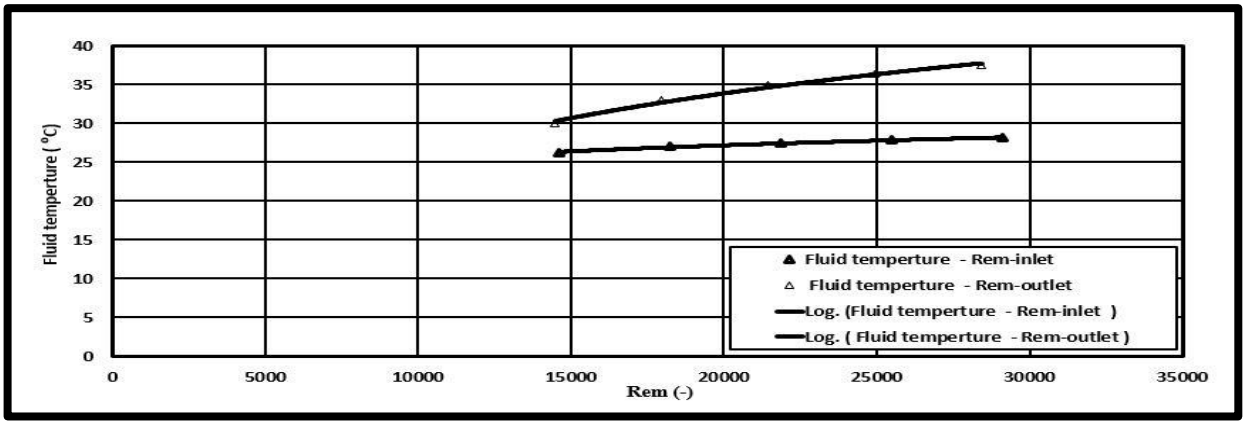


Figure 5. Depicts the correlation between the variation fluid temperature the (T_m) and wall temperature (T_w).

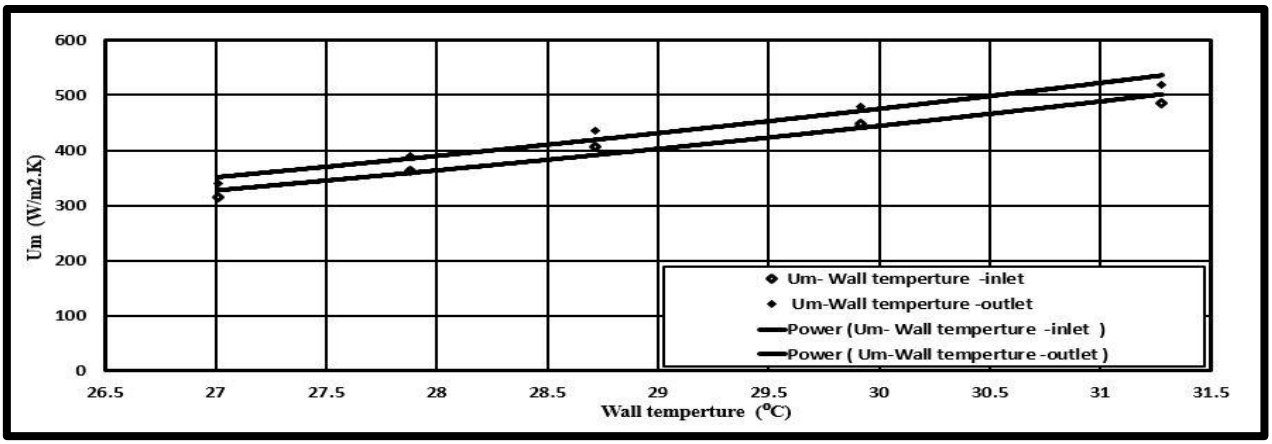


Figure 6. Coefficient of Heat transfer against wall temperature

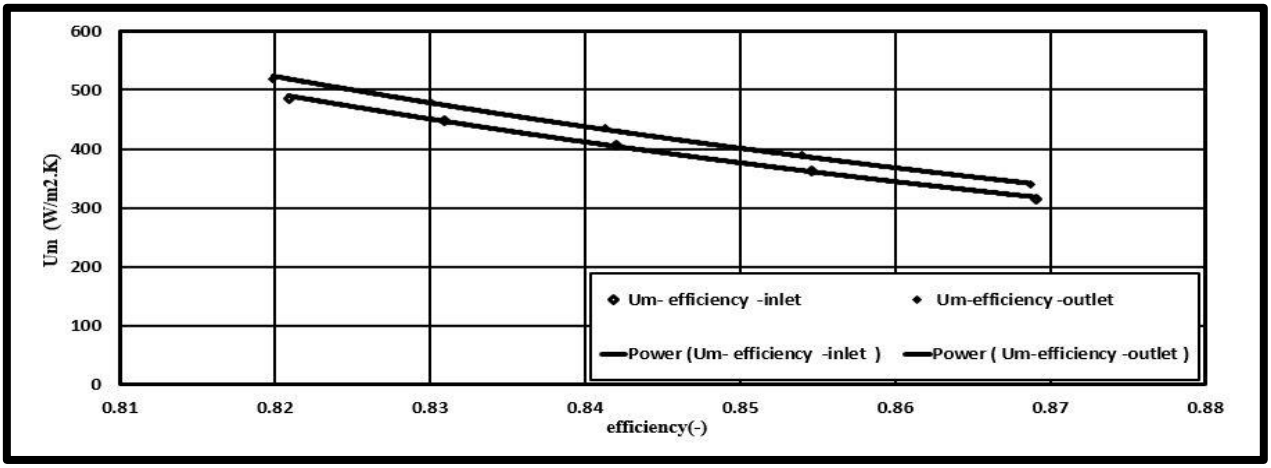


Figure 7. Coefficient of heat transfer against efficiency

Nomenclature

A_F	Total area of fin (mm2)
A_O	Tube outside area per fin pitch (mm2)
A_m	Tube heat area (mm2)
A_R	Area ratio of fin(mm2)
DO_{fin}	space between two fins (mm)
DO_m	Outer diameter (mm)
D_{hm}	Hydraulic diameter (mm)
H_f	Fin height (mm)
m_m	Mass flow rate (Kg/sec)
L_{tube}	The length of tube (mm)
N_{tube}	The numberof tube $(-)$
R_{fin}	Fin radius (mm)
Th_m	Tube Thickness (mm)
Y_f	Distance between fins (mm)
Y_{tb}	Square pitch (m)
U_m	The overall coefficient of heat transfer $/m2.K)$
Greek Symbol	
α_m	The coefficient of heat transfer (W $/m2.K)$
δ_f	Fin thichness (mm)
ρ_m	Density of fluid (Kg/m3)
μ_m	Dynamic viscosity $(N.s/m^2)$

References

[1] J. P. Holman, Heat Transfer (Si Units) Sie. Tata McGraw-Hill Education, 2008.

[2] R. SHAKIR, "GUESS HEAT TRANSFER COEFFICIENT OF FORCED CONVECTION FOR SINGLE-PHASE FLOW IN A SINGLE-PHASE PASSAGE ON A VERTICAL TUBE HEAT TRANSFER," Journal of Optimization and Decision Making, vol. 2, no. 1, pp. 139–146, 2023.

[3] R. SHAKIR, "Investigate the Flow of Boiling Heat Transfer in a Complex Geometry Flat Channel," University of Thi-Qar Journal for Engineering Sciences, vol. 12, no. 1, pp. 21–25, 2022.

[4] R. Shakir, "Valuation and Guess Single-phase transition to turbulent Developing Flows and Pressure Drop in a Copper Horizontal Pipe Heat Transfer by Using the Iterative Theory," Alkut university college journal, vol. 2025, no. بحوث مؤتمر العلمي الدولي السادس للابداع والابتكار للمدة 17-16 نيسان 2025, pp. 790–800, 2025, [Online]. Available: https://js.alkutcollege.edu.iq/article_24899.html

[5] R. Shakir, A. M. Alsayah, R. H. Rasheed, M. A. Alkhafaji, S. Algburi, and H. B. Al Husseini, "The calculation of air heat flow for finned tubes on iteration method by using heat transfer correlations:(prediction study)," in AIP Conference Proceedings, 2026, vol. 3379, no. 1, p. 30029.

[6] R. Shakır, "Design and Analytical Investigation of a Parallel-Flow Plain Shell-Pipe Heat Exchanger Considering Pressure Losses," Turkish Journal of Engineering, vol. 10, no. 3, pp. 885–892, 2026.

[7] R. Shakir, "Investigation of Single-Phase Flow Characteristics in an Inline Pin-Fins Complex Geometry," Journal of Physics: Conference Series, vol. 1879, no. 3, p. 32118, 2021, doi: 10.1088/1742-6596/1879/3/032118.

[8] R. Shakir and R. SHAKIR, "Study on Heat Transfer and Pressure Drop through Different Channel Heights and Widths," Alkut university college journal, vol. 2024, no. spacial issue, pp. 523–531, 2024.

[9] R. Shakir, "Prediction study of the boiling flow of heat transfer in an array of in-line micro-pin-fins heat sink," in AIP Conference Proceedings, 2023, vol. 2845, no. 1.

[10] R. Shakir, "INVESTIGATION OF SINGLE-PHASE FLOW CHARACTERISTICS IN A STAGGER PIN-FINS COMPLEX GEOMETRY," Journal of Engineering and Sustainable Development, vol. 25, no. 6, pp. 74–81, 2021.

[11] R. Shakir, "Study Of Pressure Drop and Heat Transfer Characteristics Of Mini-Channel Heat Sinks," the Iraqi Journal for Mechanical and Materials Engineering, vol. 22, no. 2, pp. 85–97, 2022, doi: 10.32852/iqjfmme.v22i2.595.

[12] R. Shakir, S. Algburi, and M. A. Alkhafaji, "The calculation of the heat path on the heat exchanger with the iteration method by using heat transfer equations (prediction study)," in AIP Conference Proceedings, 2025, vol. 3303, no. 1.

[13] F. A. Kareem et al., "Numerical and prediction study of the parallel micro-channels for CPU heat sink cooling," in AIP Conference Proceedings, 2026, vol. 3379, no. 1, p. 30027.

[14] A. M. Alsayah et al., "Experimental analysis study of inline square micro-pin-fins for CPU heat sink cooling," in AIP Conference Proceedings, 2026, vol. 3379, no. 1, p. 30028.

[15] S. R. Nashee, "Numerical Study for Fluid Flow and Heat Transfer Characteristics in a Corrugating Channel.," International Journal of Heat & Technology, vol. 41, no. 2, 2023.

[16] S. R. Nashee, "Enhancement of Heat Transfer in Nanofluid Flow Through Elbows with Varied Cross-Sections: A Computational Study.," International Journal of Heat & Technology, vol. 42, no. 1, 2024.

[17] A. M. Alsayah, J. J. Faraj, and A. A. Eidan, "Improvements of heat transfer coefficient for thermosiphon heat pipe heat exchanger," in AIP Conference Proceedings, 2024, vol. 3105, no. 1.

[18] R. H. Hashim, S. H. Hammdi, A. A. Eidan, A. M. Alsayah, and D. M. Abdulridh, "Performance enhancement of air-conditioning system using heat pipe heat exchanger," in AIP Conference Proceedings, 2024, vol. 3105, no. 1.

[19] R. Shakır, “POOL BOILING IN A VERTICAL ANNULUS BY A CIRCULAR PLAIN COPPER TUBE HEAT TRANSFER,” International Journal of Engineering Science and Application, vol. 9, no. 3, pp. 13–20, 2025.
[20] R. SHAKIR, “PREDICTION OF THE COEFFICIENT ON HEAT TRANSFER FOR HEAT TRANSFER FOR SINGLE-PHASE FLoW IN A ANNULAR PASSAGE ON VERTICAL TUBE BY FORCED CONVECTION HEAT FLOW,” Journal of Optimization and Decision Making, vol. 2, no. 2, pp. 297–303, 2023.
[21] R. Shakır, “PREDICTION OF THE COEFFICIENT ON HEAT TRANSFER FOR HEAT TRANSFER FOR SINGLE-PHASE FLoW IN A ANNULAR PASSAGE ON VERTICAL TUBE BY FORCED CONVECTION HEAT FLOW,” Journal of Optimization and Decision Making, vol. 2, no. 2, pp. 297–303, 2023.
[22] B. K. Dutta, Heat transfer: principles and applications. PHI Learning Pvt. Ltd., 2023.
[23] M. S. Mohammed et al., “Atmospheric water harvesting: A comprehensive review of techniques, innovations, systems, and future prospects,” Next Energy, vol. 12, p. 100731, 2026, doi: https://doi.org/10.1016/j.nxener.2026.100731.
[24] M. S. N. Kazi, Heat Transfer: Fundamentals, Enhancement and Applications. BoD–Books on Demand, 2023.